**Structural Engineering and Mechanics**, *Vol. 56, No. 3 (2015) 355-367*
DOI: http://dx.doi.org/10.12989/sem.2015.56.3.355 

# Bolted joints for single-layer structures: numerical analysis of the bending behaviour

A. Lopez- Arancibia[*1], A.M. Altuna-Zugasti[1], H. Aizpurua Aldasoro[2] and A. Pradera-Mallabiabarrena[1]

[1]*Department of Mechanical Engineering, Institute of Civil Engineering, Tecnun (University of Navarra), Manuel de Lardizábal 13, 20018 San Sebastián, Spain*
[2]*Institute of Steel Structures, Technische Universität Carolo-Wilhelmina Braunschweig, Beethovenstr. 51, 38106, Braunschweig, Germany*

*(Received December 4, 2014, Revised August 14, 2015, Accepted October 20, 2015)*

**Abstract.** This paper deals with a new designed joint system for single-layer spatial structures. As the stability of these structures is greatly influenced by the joint behaviour, the aim of this paper is the characterization of the joint response in bending through Finite Element Method (FEM) analysis using ABAQUS. The behaviour of the joints studied here was influenced by many geometrical factors, such as bolts and plate sizes, distance between bolts and end-plate thickness. The study comprised five models of joints with different values of those parameters. The numerical results were compared to the results of previous experimental tests and the agreement was good enough. The differences between the numerical and experimental initial stiffness are attributed to the simplifications introduced when modelling the bolt threads as well as the presence of residual stresses in the test specimens.

**Keywords:** joint-rigidity; single-layer structures; finite element method; nonlinear analysis; bolt connection; ABAQUS

## 1. Introduction

In the last years single-layer structures have become an appropriate and desired structural solution, especially due to their adaptability and their pleasant aesthetics (Knippers and Helbig, 2009). It is well known that joints play an important role in the stability of these structures (Wu *et al*. 2014, Zhang and Han 2013). In fact, as was shown by Altuna-Zugasti *et al*. (2012), slight improvements in joint-rigidity can make important changes in the structural behaviour. Ma *et al*. (2015) have also examined the influence of joint-rigidity on the performance of a single-layer cylindrical reticulated shell with semi-rigid joints.

The amount of research in joints for steel framed structures is huge. It would be enough to refer to the complete review written by Díaz *et al*. (2011), or to the bibliography presented by Mackerle (2003). One major point in the literature is the evaluation of the resistant capacity of the joints. But recently, as Eurocodes (EN-1993-1-8 2005) introduced the concept of semi-rigid joints, a lot of

*Corresponding author, Ph.D., E-mail: alopez@tecnun.es


http://www.techno-press.org/?journal=sem&subpage=8 ISSN: 1225-4568 (Print), 1598-6217 (Online)

research focuses precisely on the study of joint-rigidity, represented by the curve of bending moment versus rotation. Many have estimated joint-rigidity using theoretical, experimental or FEM analyses or using the component method (Shi *et al*. 2007, Mohamadi-Shooreh and Mofid 2008, Lemonis and Gantes 2009). Others, as Wang *et al*. (2013), have developed energy-based methods for the same purpose. But, irrespective of the method, it is clear that only a precise assessment of the joint-rigidity can lead to an accurate estimation of the internal forces in the members.

In contrast to the extensive research on joints for steel framed structures, there is less research devoted to the understanding of the behaviour of joints for spatial structures with tubular members (Fan *et al*. 2012). And, a great deal of this research is on double-layer structures where the role of joint-rigidity is less significant (Doh *et al*. 2009, Ghasemi *et al*. 2010 and Bezerra *et al*. 2009). Regarding single-layer structures, some researchers as the group of Shiro Kato (Hiyama *et al*. 2000) have profusely investigated structures with bolt-ball joints, where structural members are attached to the spherical joint by means of just one bolt. Others have studied more proper joints for single-layer structures, such as welded joints (Kim *et al*. 2008) or bolted joints that achieve enough rigidity because each member is attached to them by means of two bolts (Hwang 2010, Stephan *et al*. 2010). Most of the abovementioned papers combine experimental and FEM analyses.

The aim of this work is the characterization of the behaviour of a new type of bolted joint for single-layer spatial structures through FEM analysis and, for this purpose, ABAQUS is employed. The FEM model was validated comparing the results with previous experimental tests carried out by Lopez *et al*. (2011). Once a FEM model proves to perform well, it can be used for further purposes such as diagnosing zones with stress concentrations or identifying the best zones to locate strain-gauges in future tests.

## 2. Finite element modelling

### *2.1 Description of the joints*

The company that manufactures the joints is a leading engineering company in Spain which has been building large span double-layer spatial structures for many decades (Makowsky 2002). The need to be more competitive introduced the company into the single-layer spatial structures design. But the change to single-layer spatial structures implies a challenge in the design of the joints, which should be able to carry moments. The company chose to keep bolted joints, very similar to the ball joints they have always worked with. In fact, their joint, the ORTZ joint, is protected by a patent and is known world-wide (Ali *et al*. 2013). This joint has many advantages during the erection of the structure thanks to the fact that the high-strength (Grade 10.9) bolts have two parts with opposite threads of different sizes. Thus, the new joints keep the same bolts but with some changes: the cross-section of the tubes is not circular, bur rectangular; and there are two bolts at each end of the structural members, instead of only one. The joint is no longer a ball, but a cylinder, where the two bolts of each member attach. Fig. 1 shows a sketch of the actual joint for single-layers with the cylinder and the two bolts. The moment capacity depends on the separation between the two bolts “h”. The plan view in Fig. 1 looks almost like the sectional view of the ORTZ ball-joint. The circular tubes for the ORTZ system had a conical end. In the new concept, the heads of the bolts lie on a plate welded at the ends of the rectangular hollow tubes. Some specimens ready for the experimental tests can be seen in Fig. 2.

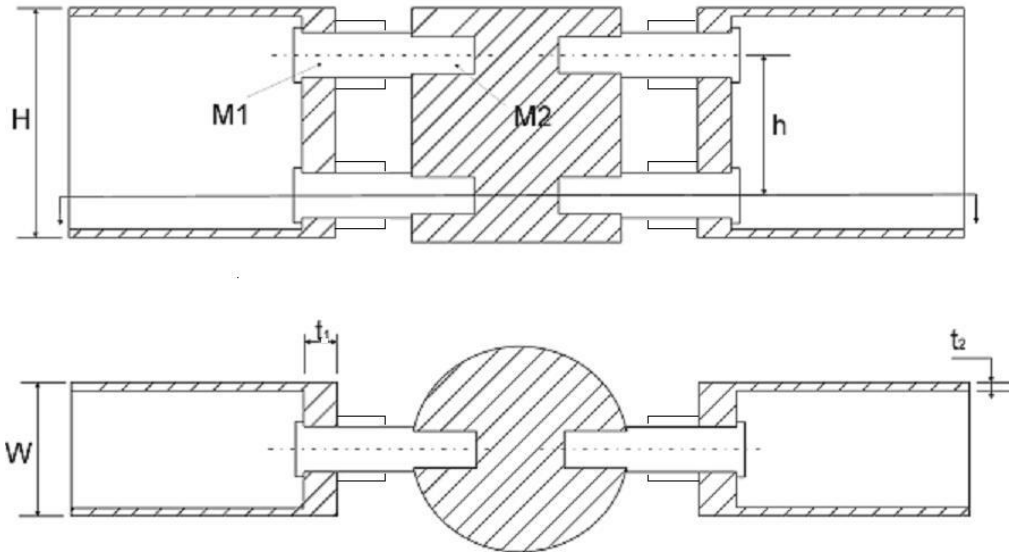


Fig. 1 Sketch of the joint: lateral and plan view

Fig. 2 Some specimens before the experimental tests

Among the different tests that were carried out to check the new design, the characteristic of the joint that will be more relevant for the behaviour of the structure is the bending stiffness, which was measured by means of four-point bending tests (Fig. 3). Experimental work is necessary, but it is expensive. Besides, there are relevant areas in the specimens where measurements are limited, due to accessibility difficulties. If the joints can be analysed numerically, the FEM models will be a great aid during the joint design and verification process.

Table 1 shows the geometrical details of the different specimens analysed with FEM. As mentioned before, the bolts have two parts of different sizes, where M1 and M2 are the two nominal diameters. Apart from the geometrical details, Table 1 also lists critical loads for the

Fig. 3 Four-point bending experimental test of the joint system

Table 1 Details of the specimens (dimensions in mm)

| Specimen | Beam Section ($H \times W \times t_2$) | Plate thickness ($t_1$) | Bolt metric (M1-M2) | Bolt distance ($h$) | $P_{y,\,bolt}$ (kN) | $(P_{pl,\,tube})/(P_{u,bolt})$ |
|---|---|---|---|---|---|---|
| A | 140×80×4 | 15 | 16-20 | 98 | 13.6 | 1.57 |
| B | 140×80×5 | 20 | 22-27 | 84 | 22.4 | 1.15 |
| C | 140×80×6 | 20 | 22-27 | 84 | 22.4 | 1.32 |
| D | 140×80×6 | 25 | 30-36 | 70 | 34.6 | 0.86 |
| F | 200×100×6 | 25 | 30-36 | 122 | 61.6 | 0.98 |

bending tests, which were estimated under the simplified assumption that the bending moment of the tube is transmitted at the bolts by positive tension of one bolt and compression of the other one. In Table 1, $P_{y,bolt}$ is the amount of total load required from the hydraulic actuator to reach the yield stress in the tension bolt, whilst $(P_{pl,tube})$ / $(P_{u,bolt})$ indicates the ratio of the load required for plastic failure of the tube in bending to the ultimate load of the tension bolt. This ratio takes values greater or less than unity depending mainly on the choice of "$h$" and on the distance between the supports.

### *2.2 Finite element model*

The FEM model replicates the different details of the real system, such as the multiple changes of diameter that take place along the bolt. However, the thread of the bolt was not modelled because the labour it takes is not rewarded with a significant improvement in the results. In fact, there is never information about the gaps between the two threads in contact before the system is loaded, so the exact modelling of the thread is not worthy. Nevertheless, the numerical models were able to follow very closely the experimental results.

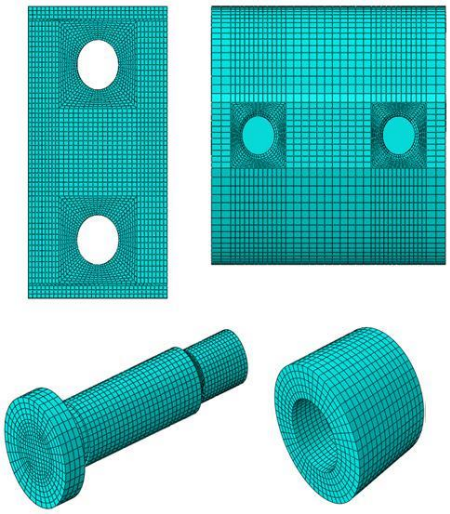

Fig. 4 Finite element meshes of the joint components

Table 2 Material properties for the models in ABAQUS

| Element | Data point | True stress (MPa) | True plastic strain |
|---|---|---|---|
| Steel core | 1 | 450.9 | 0 |
| | 2 | 450.9 | 0.050 |
| | 3 | 800.4 | 0.085 |
| Tube | 1 | 356.3 | 0 |
| | 2 | 416.7 | 0.014 |
| Bolts | 1 | 905.9 | 0 |
| | 2 | 1016.3 | 0.011 |

A great effort was done instead in achieving a tidy mesh, with adequate values for element skewness and aspect ratio. Finer meshes were used in the elements that take part in the contact interactions, where high stress and strain gradients were expected to occur. Fig. 4 shows the refined meshes for nuts, for bolts and for the relevant zones of the end-plate and the central core. Eight-node linear brick elements (C3D8) were used. Reduced order integration was activated for all the elements involved in the interactions (Fu *et al.* 2008) in order to prevent shear locking which can occur with C3D8. The C3D8 mesh could also overestimate the rigidity of the joint, as described by Hibbitt and Sorensen (2008).

### *2.3 Material model*

The von Mises yield criterion with isotropic hardening rule was used to model the steel components. Material non-linearity was included in the finite element model by multilinear stress-strain curves, as Abolmaali *et al.* (2005). Material properties were defined in ABAQUS in terms of true value of stress and plastic strain, following the procedure in Fu *et al.* (2008). The value for the elastic Young's modulus was taken as 200 GPa and Poisson's ratio was set to 0.3. The nuts and the bolts were made of high-resistant steel. As shown in Table 2, the rest of materials were less resistant but more ductile.

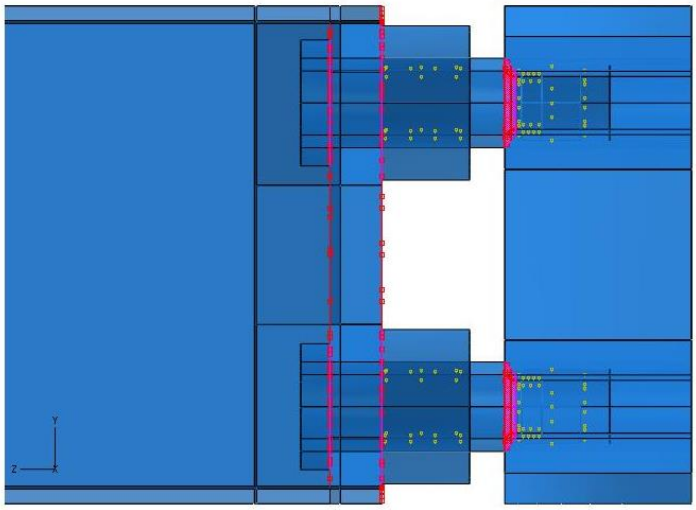

Fig. 5 Surface contacts in FEM model

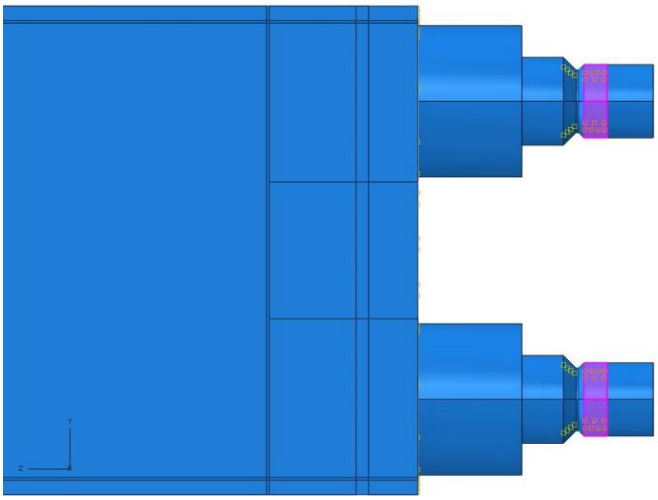

Fig. 6 Tie constraint between bolt and central core

### *2.4 Interactions*

A good representation of the contacts between elements has huge effects in the response of the connections and in the behaviour of the whole system. In this particular joint, the bolt is the element that connects the different components. Both, the bolt and the nuts, are in contact with the end-plate and the cylindrical core. Consequently, contact surfaces were defined in the following areas, which are represented by dots in Fig. 5:

- The head of the bolt which is in contact with the inner surface of the end-plate.
- The nut which is in contact with the outer surface of the end-plate.
- The bolt-chamfer which lies on the steel core.

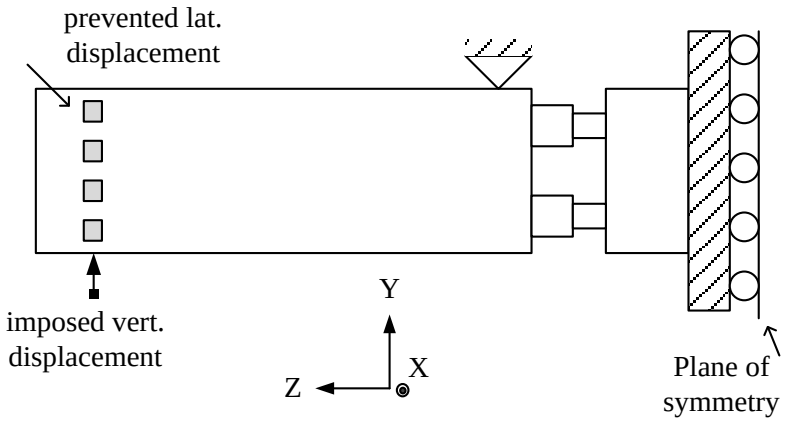


Fig. 7 Sketch of FEM model with boundary conditions

An accurate model for the contacts implies taking into account both normal and frictional forces. Concerning frictional forces, the usual value for the Coulomb coefficient in the literature is 0.33. However this value can vary from 0.1, for lower frictional force, up to 0.5. Here, the maximum value of 0.5 was chosen as it is the value recommended for bolts of Grade 10.9 (Ortiz *et al.* 2009). Nevertheless, friction does not play a significant role in this specific joint configuration.

Another critical detail in the model is the modelling of the bolt thread. It was decided to neglect the detailing of the threads and to simulate their effects by means of a TIE constraint instead. This kind of constraint makes equal all the degrees of freedom of the nodes of both surfaces. So, TIE constraints were applied to connect the bolts with the nuts and also to attach the bolts to the central core. In the latter connection, the TIE was defined only for 25% of the bolt length because most of the bolt force is concentrated in this area (Bickford 1995). The TIE contact surface is coloured in pink in Fig. 6.

The interactions were solved in ABAQUS with a master-slave type algorithm. Bolts, being the stiffer components, were always taken as master surfaces. The corresponding slave surfaces were accordingly meshed with finer meshes.

### *2.5 Boundary conditions and loads*

Since the configuration of the four-point bending test is symmetrical, only half of the system was modelled in FEM. The simply supported specimen is reduced to just half of it with clamped conditions at the plane of symmetry. The only movement that is not restrained at that plane is the vertical (*Y*) displacement (Fig. 7). The numerical analyses were carried out with a displacement control, because this control method is more robust and the analysis converges better than with the force control. Consequently, the progress of the analysis was controlled by the vertical displacement imposed at the nodes that corresponds to the supports in the real experiment. Logically, the vertical displacement was prevented for the line where the load is applied in the experimental test. And finally, lateral (*X*) displacements were restrained at the end of the tube, as they were in the real test.

## 3. Results of FEM and comparison with the experimentation

### 3.1 Load-displacement curves

Although the FEM models will be very useful for many studies, the comparison between the FEM results and the experimentation has to be done in terms of the load-displacement curves. These curves were the direct outcome of the experimental tests and can be afterwards changed into moment-rotation curves, which are the curves used by EN 1993-1-8 to classify the stiffness of joints.

The numerical and experimental curves are plotted in Figs. 8 (a)-(e). The curves have a bilinear general shape, with a change in slope that occurs at approximately $P_{y,bolt}$ (Table 1). The numerical models picked up the general behaviour of the joint in the tests, although they showed a slightly stiffer initial slope. The reason for this discrepancy is that the numerical models were not able to reproduce exactly some details such as initial gaps between threads or residual stresses. Nevertheless, the numerical curves are close enough to the experimental ones especially taking into consideration that the study comprised joints of different characteristics, as it is the case of Specimens D and F, which are compared in the following section. On the contrary, Specimens B and C only differ in the tube thickness. Thus, their behaviour is almost the same (Figs. 8(b) and 8(c)) except that Specimen B, with a thinner tube, is slightly more flexible. In fact, this little influence of the tube capacity in Specimens B and C is in consonance with the fact that, for these two joints, the critical element is clearly the bolt in tension, as shown by the ratio of loads in the last column of Table 1.

### 3.2 Critical elemement for the resistance capacity of the joint

The FEM models reproduced the experimental failure modes of the real joints. As predicted by the values in the last column of Table 1, in the experimental tests the failure of Specimens A, B and C was due to failure of the tension bolt. That was also the behaviour showed by the FEM analyses. The tension bolts of the three specimens reached the ultimate strength, as can be seen in the Von Mises stress plot (Figs. 9, 10 and 11). Stress plots in this paper correspond to the last point

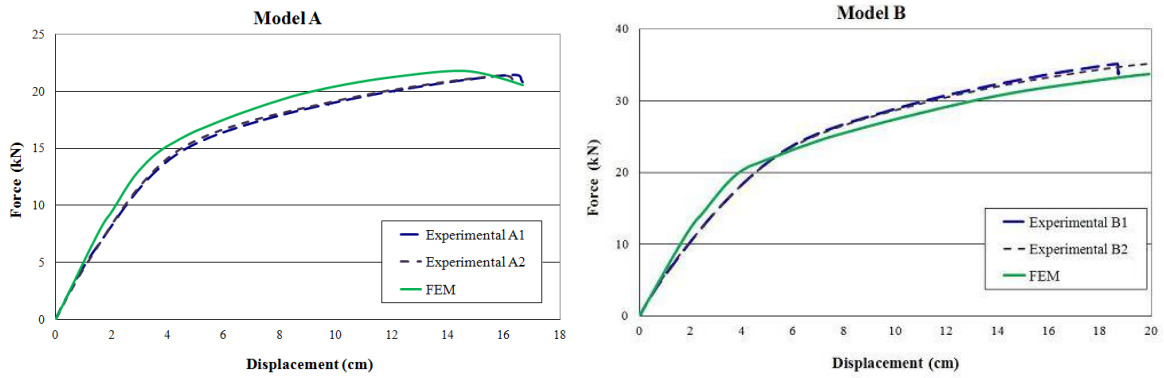


(a) Model of Specimen *A* (b) Model of Specimen *B*

Fig. 8 Comparison between FEM and experimental load-displacement curves

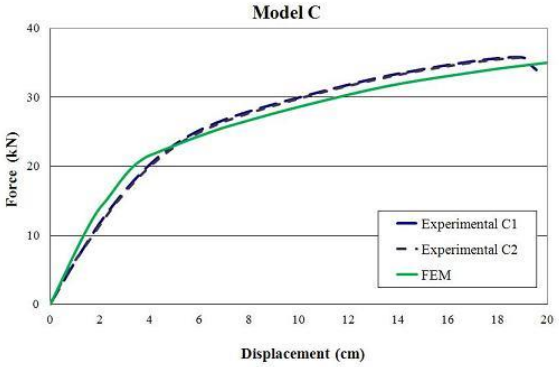


(c) Model of Specimen *C*

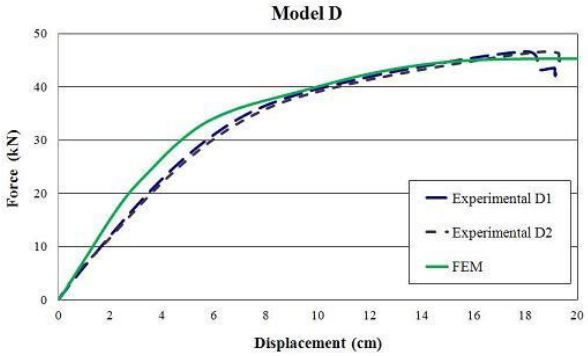


(d) Model of Specimen *D*

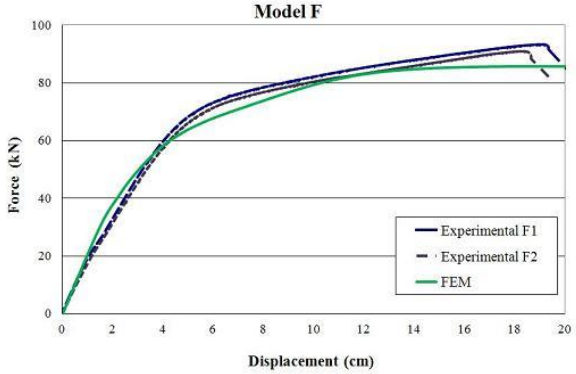


(e) Model of Specimen *F*

Fig. 8 Continued

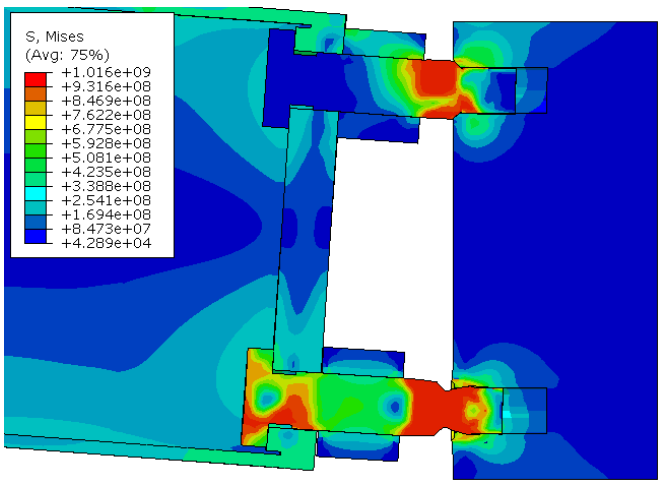


Fig. 9 Stress plot for Specimen *A* at the middle plane

of the FEM curve in Fig. 8. For these three joints, the stress plots show that the bolt in tension had stress concentration at the smallest section and the corresponding nut lost contact with the end-

plate. The steel core almost reached the ultimate stage of material capacity (800.4 MPa) in the interaction with the bolt. The bolt in compression was forced into the central core, causing stress concentration at the point where the contact took place. At the same time, the end-plate suffered large deformation in the experimental tests, and the same behaviour was shown in the numerical analysis.

For Specimen *D*, the ratio between the two failure loads in Table 1, $P_{pl,tube}$ /$P_{u,bolt}$, is less than one. Therefore, in this case, it is expected that the plastic bending moment of the tube is reached before the tension bolt fails, and so it happened in the experimental test (Fig 12). For Specimen *F* all the geometrical values were the same as for Specimen *D*, except the beam height and the separation between bolts. As a result, Specimen *F* had relatively smaller bolts and this fact lead to failure of the bolt in tension (Fig. 13), although the prediction for Specimen *F* was that both elements, tube and bolt, had similar critical loads. The stress plots for these two specimens with such a different behaviour show that the FEM models were able to reproduce the experimental tests. In the stress plot for Specimen *D* (Fig. 14) the bolts are far from the critical stress. So, it is

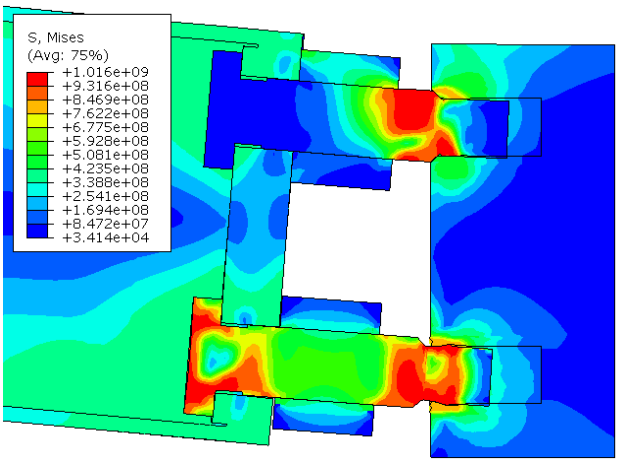


Fig. 10 Stress plot for Specimen *B* at the middle plane

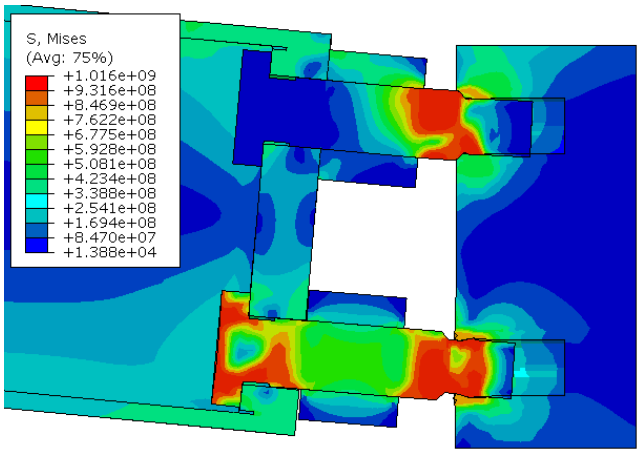


Fig. 11 Stress plot for Specimen *C* at the middle plane

Fig. 12 Tube failure in Specimen *D*

Fig. 13 Bolt fracture in Specimen *F*

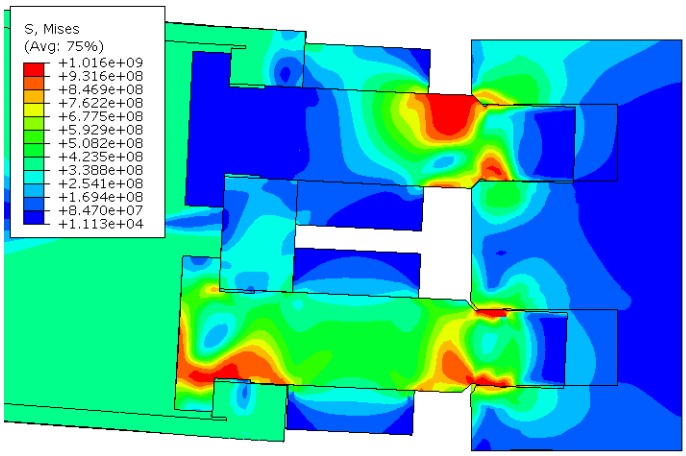


Fig. 14 Stress plot for Specimen *D* at the middle plane

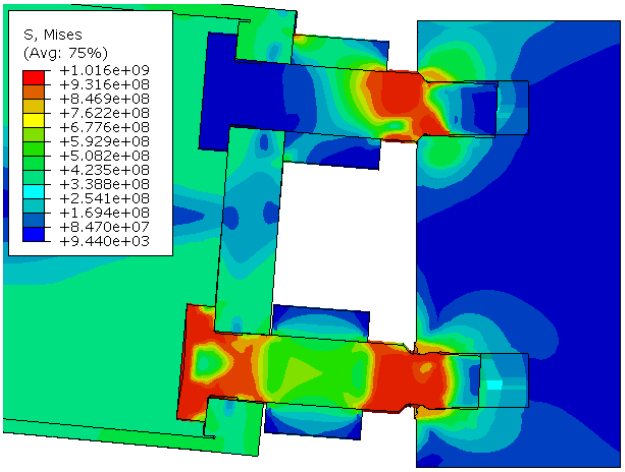


Fig. 15 Stress plot for Specimen *F* at the middle plane

clear that the limit in the final capacity of the load-displacement curve is due to yielding of the tube. The stress plot for Specimen *F* (Fig. 15) shows that both elements, tube and bolt, are close to their limit.

## 4. Conclusions

3-D finite element analyses were carried out to study the behaviour of semi-rigid joints, when subjected to four-point bending tests. The commercial software ABAQUS facilitates an accurate modelling of difficult details, such as contacts and other interactions. Although complex and time-consuming, the finite element analyses provide very useful information for the actual behaviour of the system and for further developments. In this work, the results were compared with experimental data in order to validate the FEM models. The correlation between both responses was quite acceptable especially considering that the study deals with the behaviour of joints with very different relative sizes. The differences between the numerical and experimental initial stiffness are attributed to the simplifications introduced when modelling the bolt threads as well as the presence of residual stresses in the test specimens.

## References

Abolmaali, A., Matthys, J.H., Farooqi, M. and Choi, Y. (2005), "Development of moment-rotation model equations for flush end-plate connections", *J. Constr. Steel. Res.*, **61**(12), 1595-1612.

Ali, M.I., Fan, F., Khakina, P.N. and Ma, H.H. (2013), "Cost-effective design of space structures joints: a review", *Int. J. Civ. Arch. Struct. Constr. Eng.*, **7**(1), 21-25.

Altuna-Zugasti, A.M., Lopez-Arancibia, A. and Puente, I. (2012), "Influence of geometrical and structural parameters on the behaviour of squared plan-form single-layer structures", *J. Constr. Steel Res.*, **72**, 219-226.

Bezerra, L.M., de Freitas, C.A.S., Matias, W.T. and Nagato, Y. (2009), "Increasing load capacity of steel space trusses with end-flatenned connections", *J. Constr. Steel Res.*, **65**(12), 2197-2206.

Bickford, J.H. (1995), *An Introduction to the Design and Behavior of Bolted Joints*, Ed. M. Dekker, New York, NY, USA.

Díaz, C., Marti, P., Victoria, M. and Querin, O.M. (2011), "Review on the modelling of joint behavior in steel frames", *J. Constr. Steel Res.*, **67**(5), 741-758.

Doh, J., Kin, J. and Park, M.H. (2009), "Analysis and experiments for form finding of the SCST structures", *Proceedings of the International Association for Shell and Spatial Structures (IASS) Symposium*.

EN 1993-1-8 (2005), *Eurocode 3: Design of steel structures, Part 1-8: Design of joints*, Brussels, Belgium.

Fan, F., Ma, H., Chen, G. and Shen, S. (2012), "Experimental study of semi-rigid joint systems subjected to bending with and without axial force", *J. Constr. Steel Res.*, **68**(1), 126-137.

Fu, F., Lam, D. and Ye, J. (2008), "Modelling semi-rigid composite joints with precast hollowcore slabs in hogging moment region", *J. Constr. Steel Res.*, **64**(12), 1408-1419.

Ghasemi, M., Davoodi, M. and Mostafavian, S. (2010), "Tensile stiffness of mero-type connector regarding bolt tightness", *J. Appl. Sci.*, **10**, 724-730.

Hibbitt, K. and Sorensen, E.P. (2008), *ABAQUS 6.8: A computer software for finite element analysis*, Hibbitt and Sorensen Inc, Rhode Island, RI, USA.

Hiyama, Y., Takashima, H., Iijima, T. and Kato, S. (2000), "Buckling behaviour of aluminum ball jointed single layered reticular domes", *Int. J. Space Struct.*, **15**(2), 81-94.

Hwang, K. (2010), "Advanced investigations of grid spatial structures considering various connection systems", Ph.D. Dissertation, University of Stuttgart, Stturgart.

Kim, Y., Lee, Y. and Kim, H. (2008), "Bending test of welded joints for single-layer latticed domes", *Int. J. Steel Struct.*, **8**, 357-367.

Knippers, J. and Helbig, T. (2009), "Recent developments in the design of glazed grid shells", *Int. J. Space Struct.*, **24**(2), 111-126.

Lemonis, M.E. and Gantes, C.J. (2009), "Mechanical modeling of the nonlinear response of beam-to-column joints", *J. Constr. Steel Res.*, **65**(4), 879-890.

Lopez, A., Puente, I. and Aizpurua, H. (2011), "Experimental and analytical studies on the rotational stiffness of joints for single-layer structures", *Eng. Struct.*, **33**(3), 731-737.

Ma, H., Fan, F., Wen, P., Zhang, H. and Shen, S. (2015), "Experimental and numerical studies on a single-layer cylindrical reticulated shell with semi-rigid joints", *J. Constr. Steel Res.*, **86**, 1-9.

Mackerle, J. (2003), "Finite element analysis of fastening and joining: a bibliography (1990-2002)", *Int. J. Press. Ves. Pip.*, **80**, 253-271.

Makowski, Z.S. (2002), "Development of jointing systems for modular prefabricated steel space structures", *Lightweight Structures in Civil Engineering, Proceedings of the IASS International Symposium*, 17-41.

Mohamadi-Shooreh, M. and Mofid, M. (2008), "Parametric analyses on the initial stiffness of flush end-plate splice connections using FEM", *J. Constr. Steel Res.*, **64**(10), 1129-1141.

Ortiz, J., Hernando, J.I. and Cervera, J. (2009), *Manual de Uniones Atornilladas Laterales*, Publicaciones APTA, Madrid, Spain. (in Spanish)

Shi, Y., Shi, G. and Wang, Y. (2007), "Experimental and theoretical analysis of the moment-rotation behavior of stiffened extended end-plate connections", *J. Constr. Steel Res.*, **63**(9), 1279-1293.

Stephan, S., Pan, F. and Huang, Y. (2010), "The freeform structure of the UAE pavilion at the Shanghai EXPO 2010", *Proceedings of the International Association for Shell and Spatial Structures (IASS) Symposium*.

Wang, S., Zhang, M. and Liu, F. (2013), "Estimation of semi-rigid joints by cross modal strain energy method", *Struct. Eng. Mech.*, **47**(6), 757-771.

Wu, H., Zhang, C., Gao, B. and Ye, J. (2014), "Theoretical and experimental study of robustness based design of single-layer grid structures", *Struct. Eng. Mech.*, **52**(1), 19-33.

Zhang, H. and Han, Q. (2013), "A numerical investigation of seismic performance of large span single-layer latticed domes with semi-rigid joints", *Struct. Eng. Mech.*, **48**(1), 57-75.